

Research Article

Statistical analysis of the theoretical geometric-kinematic surface roughness model at turning

Suratjon Nuriddinov¹, Balázs Mikó^{2,*}

¹Doctoral School of Material Science and Technology, Óbuda University
Népszínház u. 8, 1081 Budapest, Hungary

²Institute of Mechanical Engineering and Technology, Óbuda University
Népszínház u. 8, 1081 Budapest, Hungary

*e-mail: miko.balazs@bgk.uni-obuda.hu

Submitted: 05/09/2025 Accepted: 05/12/2025 Accepted: 10/12/2025 Published online: 12/02/2026

Abstract: Manufacturing methods can produce precision machined parts where surface roughness is an important performance characteristic, affecting fatigue strength, corrosion resistance, and aesthetics. Achieving ideal surface roughness is complex, influenced by tool-material interactions and machine conditions. Predicting surface roughness has high importance in machine design and manufacturing process planning. Key approaches include: machining theory (analytical models using cutting parameters), data analysis (empirical/statistical methods), designed experiments, AI, and image processing. The article presents a geometric-kinematic surface roughness model, and based on it the standard surface roughness parameters are determined. The arc based profile model is used, and the model makes possible to use a statistical analysis based improvement method in order to increase the accuracy of the prediction. The theoretical model, the process of the calculation and the regression analysis of the model is presented.

Keywords: turning; surface roughness; prediction model; geometric approach; equivalent replacement profile

I. INTRODUCTION

Machining is a process used to create a part or shape with precise dimensions and tolerances. Surface roughness plays a crucial role in determining the quality of the product, as it directly impacts the product's performance during use. Surface roughness is a critical parameter that affects the mechanical, tribological and aesthetic properties of machine parts. The quality of the surface significantly enhances properties such as fatigue strength, corrosion resistance, and creep life. Optimizing surface roughness can result in improved performance, longer life and better overall functionality of machine parts. Understanding and controlling surface roughness is essential for the design, manufacture and maintenance of high quality machine parts [1,2].

With the increasing demand for improved surface quality, especially in industries like automotive, aerospace, and die and mould manufacturing, achieving a smooth surface finish is essential.

Surface roughness is typically measured by a specific value, where a higher value indicates a

rougher surface and a shorter fatigue life. Therefore, it's important to clearly specify the required surface roughness in designs to ensure the machining process is appropriately adjusted to meet these standards.

Achieving an ideal surface finish in machining remains a significant challenge due to the complex and interdependent interactions between the cutting tool, the workpiece material, and the machining environment. Several factors contribute to surface imperfections, including the formation of a built-up edge, which alters the effective geometry of the cutting tool; surface damage caused by chips curling back and impacting the freshly machined surface; tearing during chip formation in ductile materials; and surface cracks resulting from discontinuous chip formation in brittle materials. Friction between the tool's flank and the workpiece further degrades the surface finish. Beyond these, key machining parameters - such as feed rate, cutting speed, and depth of cut - along with the process kinematics, cutting tool geometry and material, mechanical properties of the workpiece, and dynamic issues like machine vibrations and tool deflection, play crucial roles. The precision, rigidity, and overall condition

of the machine tool itself also significantly influence surface quality.

Depending on the required accuracy, surface type, and application, different measurement techniques are used for measure surface roughness [1]. The comparative surface measurement method, when the machined surface is compared with an etalon part, is cheap, but non accurate, and it is need lot of experience. Contact methods, such as stylus profilometers, are widely adopted for their reliability and standardized out-puts, while non-contact optical methods, like interferometry and confocal microscopy, offer high-resolution analysis without risking surface damage. Advanced techniques like atomic force microscopy enable nanoscale assessments, although they are limited to small areas and specialized applications. Selecting the appropriate method depends on balancing precision needs, surface characteristics, and practical constraints such as speed and cost.

Surface roughness parameters can be classified based on measurement dimension, functional characteristics, and application relevance [1]. By dimension, they are divided into profile (2D) parameters like R_a , R_z , R_t , and areal (3D) parameters like S_a , S_z , S_q , which provide more comprehensive surface data. Functionally, parameters are grouped into amplitude parameters (e.g., R_a , R_q , S_a) that describe vertical deviations; spacing parameters (e.g., R_{sm} , S_{ds}) that define the frequency or distribution of surface features; hybrid parameters (e.g., R_{dq} , S_{dq}) combining height and spacing; and functional parameters (e.g., R_k , R_{pk} , R_{vk} , and their 3D equivalents S_k , S_{pk} , S_{vk}) used to predict behaviour under contact, lubrication, or wear. In terms of application, general parameters like R_a or S_a are used for standard quality control, while sensitive or functional parameters are selected for specific tasks where surface peaks and valleys critically influence performance, such as in sealing, friction reduction, or fatigue resistance.

The most often used profile parameters are the next:

- R_a – The arithmetical mean of the absolute values of the profile deviations from the mean line of the roughness profile.
- R_z - The average of consecutive highest peaks and lowest valleys. Vertical distance between the highest peak and lowest valley, the distance of the second highest peak and the second lowest valley, etc. This is usually done for the five biggest deviations, and then an average is calculated.
- R_q - The root-mean-square (RMS) roughness measures the square root of the average of the squared deviations from the mean line.
- R_t – The total height of the roughness profile is the distance between the highest peak and the deepest valley.

- R_p - The calculated distance between the profile's highest peak and the mean line within the evaluation length.
- R_v - The calculated distance between the profile's deepest valley and the mean line within the evaluation length.
- R_{sm} – Mean peak with is the mean value of the width of the profile elements.
- R_{sk} – The skewness values for the profile points, which measures the asymmetry of the amplitude density curve.
- R_{ku} – The kurtosis value for the profile points, which measures the peakedness of the amplitude density curve. The kurtosis value of the Gaussian curve is 3.

Predicting surface roughness in machining is critical for ensuring product quality and process optimization. Multiple approaches have been developed, each leveraging different principles, tools, and technologies [1]. There are five key approaches to sur-face roughness prediction:

Machining theory approach is based on machining theory to develop analytical models to represent the machined surface. It uses mathematical equations derived from machining geometry and mechanics to predict surface roughness. Consider parameters like feed rate, tool nose radius, cutting speed, and depth of cut [1]. Models of ten simplify real conditions and are implemented in computer algorithms for simulation and prediction. Fast and useful for early-stage design but less accurate under real-world complexities. The FEM simulation based topography generation can consider more realistic circumstances [3].

Data analysis approach examines the effects of various factors through the data collection and the analysis. Involve performing machining experiments under varying conditions to observe how different factors affect surface roughness. Empirical data is collected and analysed statistically to identify relationships. Common tools include regression analysis and ANOVA. Highly accurate for specific setups but time-consuming and limited in generalizability.

Designed experiments approach uses structured statistical methods like design of experiments (DoE), Taguchi methods, and response surface methodology (RSM) to systematically investigate multiple factors and their interactions. Allow for efficient optimization of surface roughness with systematized experiments. Provide statistically robust models but still require careful planning and execution [4].

Artificial intelligence (AI) approach applies machine learning techniques such as artificial neural networks (ANN), support vector machines (SVM), genetic algorithms, and fuzzy logic to model

complex, nonlinear relationships between input parameters and surface roughness [5]. Offer high prediction accuracy and adaptability but require large datasets and significant computational resources [6,7].

Image processing approach uses high-resolution imaging and digital analysis to extract surface texture features. Techniques include edge detection, 3D reconstruction, and texture analysis using methods like GLCM or various AI methods. Suitable for non-contact, real-time inspection in production environments. Sensitive to lighting and surface conditions, requiring robust setup and calibration [8].

[1] presents several geometric model approach for turning and milling technologies. In case of turning three basic models are presented (Fig. 1). A simple kinematic-geometric model of the surface roughness in case of turning considers the feed and the nose radius (RE). The cutting edge angle (KAPR) and the minor cutting edge angle (ECEA) may also play a role in the geometric model, depending on the value of the nose radius and the depth of cut.

The first model (Figure 1) is known as Bauer formula, which is the most often used model. The kinematic-geometric model shows some inaccuracy comparing to the real test parts. The geometric model can be improved. The value of the minimal chip thickness has influence to the the surface roughness, as the comparison of Bauer and Brammertz formulas to cutting tests results shown [9].

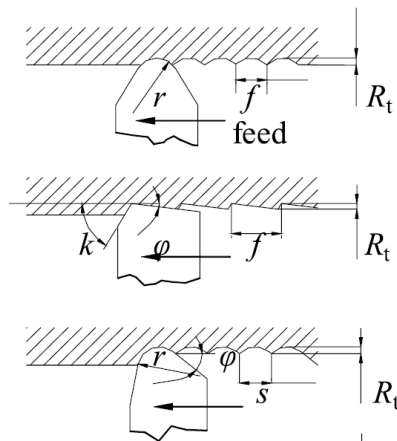


Figure 1. Kinematic-geometric surface roughness models of turning [1].

In case of turning, considering the tool face surface inclination and the rake angle, an asymmetric elliptical nose radius can be used instead of circular nose radius [10]. The ellipse can be generated by geometric transformations from the circular geometry. The accuracy of the elliptic model can be improved by regression function [11]. Power

function regression can be generated based on cutting tests.

The other way to create geometric based surface roughness model is the application of CAD simulation. In this way, not only the theoretical surface roughness can be evaluated, but the tool wear can be considered [12].

The kinematic-geometric model of the surface roughness is very similar in case of turning and milling, as [13] presents, so the models of milling method, can be relevant also. The presented model in [14], which consider the r , cutting edge angle and f , describes the same cutting situation, like turning (Fig. 2).

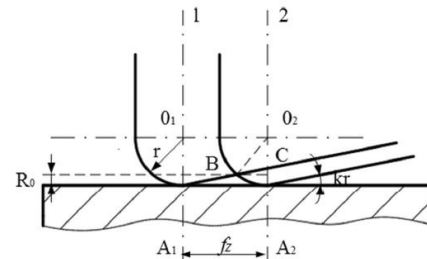


Figure 2. Kinematic-geometric surface roughness model of face milling [14].

The aim of our research is to create a geometric based surface roughness prediction model, which consider the machining and tool parameter based uncertainties. The aim of the current article is to present a kinematic-geometric surface roughness model, and based on it to determine the standard surface roughness parameters.

II. METHOD

Based on the kinematic-geometric method, the surface profile is generated by the tool geometry and the motion parameters.

When the turning tool is substituted by the corner radius (RE), the surface profile is a series of intersected arcs. Considering, the distance between two centre point is the feed (f), one section of the curve can be described by two arcs. The first arc there is between the previous intersection point and the bottom of the valley, and the second there is between the bottom of the valley and the intersection point. The x and y coordinates of the centre point and the intersection points define the constrains of the g' and g'' angular parameter of the curve sections (Fig. 3b). For the calculation, the angular range is divided into j pieces.

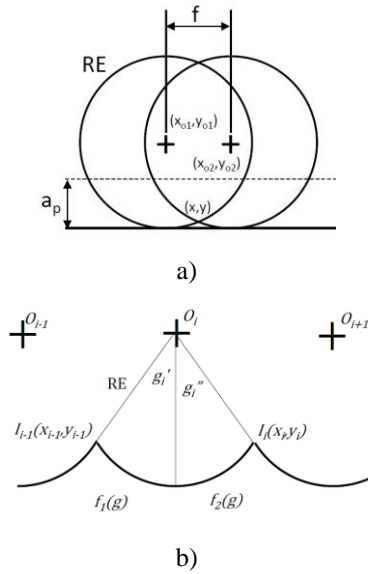


Figure 3. Geometric model of surface profile. a) Circle based model. b) Intersection points.

The points of the arcs can be described by the next equation:

$$f_1(g) = \begin{bmatrix} x_{oi} + RE \cdot \sin(-g'_i + j \cdot \delta g'_i) \\ y_{oi} - RE \cdot \cos(-g'_i + j \cdot \delta g'_i) \end{bmatrix} \quad (1)$$

where $\delta g'_i$ is the resolution unit, and the g'_i is the maximum value of the angle.

$$\delta g'_i = \frac{g'_i}{j} \quad (2)$$

$$g'_i = \arcsin \frac{x_{oi} - x_{i-1}}{RE} \quad (3)$$

The equation of the second section of the arc can be calculated similarly.

$$f_2(g) = \begin{bmatrix} x_{oi} + RE \cdot \sin(j \cdot \delta g''_i) \\ y_{oi} - RE \cdot \cos(j \cdot \delta g''_i) \end{bmatrix} \quad (4)$$

$$\delta g''_i = \frac{g''_i}{j} \quad (5)$$

$$g''_i = \arcsin \frac{x_i - x_{oi}}{RE} \quad (6)$$

In order to calculate the value of the angles, the coordinates of the intersection point are required. The coordinates of the intersection point have to be calculated as the intersection of two circles (**Fig. 3a**). The equations of these two circles are:

$$R_1^2 = (x - x_{o1})^2 + (y - y_{o1})^2 \quad (7)$$

$$R_2^2 = (x - x_{o2})^2 + (y - y_{o2})^2 \quad (8)$$

The detailed calculation can be seen in the Appendix. At the result, the coordinates of the intersection point are:

$$y_I = \frac{-b - \sqrt{b^2 - 4ac}}{2a} \quad (9)$$

$$x_I = -y_I \cdot C_3 + C_4 \quad (10)$$

The aim of this calculation is to create the point series of the theoretical surface profile. Based on these points, the surface roughness parameters can be calculated. In order to deeper analysis of the presented model, the theoretical profile was generated for different parameters. The tool corner radius (RE) and the feed (f) were varied based of full factorial plan. The values of the RE were 0.4, 0.8 and 1.2 mm, which follows the possible standard RE values of a turning insert. The feed values were between 0.1 and 0.4 mm, with 0.05 step (7 values). Based on the generated points of the theoretical surface profile the surface roughness parameters were calculated: Ra, Rz, Rq, Rt, Rp, Rv, Rsm, Rsk, Rku. Based on the RE and f the theoretical value of the surface roughness based of Bauer formula was calculated also (Rt*).

The simulated profile was compared with a real surface profile as an example. The real surface was machined by V shape turning insert (VBMT 110204-UF4315 Sandvik Coromant), on Euroturn 12B CNC turning machine ($v_c = 120$ m/min, $f=0.25$ mm, $a_p = 0.5$ mm). The material of the specimen was 42CrMo4 (1.7225) alloy steel, the surface diameter was 34 mm. The surface roughness was measured by Mitutoyo SJ-301 measuring instrument.

III. RESULTS

Table 4 in Appendix B shows the calculated data in case of different RE and f parameter values. The **Fig. 8** (Appendix B) shows the values in function of the nose radius (RE) and the feed (f). In case of height parameters, the RE has small effect on the roughness parameters when small feed. But in case of large feed, the radius has large positive effect on the surface roughness.

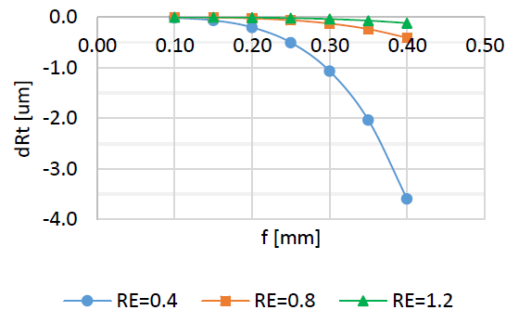


Figure 4. Difference between the Bauer formula and the presented model.

The longitudinal parameter (Rsm) depends on the feed only. The Rsk and Rku parameters have minimum point at small radius and large feed, but the differences are very small.

The result of the traditional Bauer formula and the new method can be compared at Rt. Fig. 4 shows the difference of Rt in case of the Bauer formula (Rt*) and the result of the model:

$$dRt = Rt^* - Rt \tag{11}$$

Based on the simulation data a regression analysis can be created. Three version were calculated, which contained different sets of variables. The first version contains the nose radius (RE) and the feed (f) only, the second version contains the RE, the f and the square of the f, and the third version contains the RE, the f and the predicted value of Rt based on Bauer formulae (Rt*).

The general equation of the linear regression is the next:

$$Rx = C + C_1 \cdot RE + C_2 \cdot f + C_3 \cdot f^2 + C_4 \cdot Rt^* \tag{12}$$

Table 1 shows the values of the coefficients in case of Rt parameter and the determination coefficient (R²), which shows the explanatory power of the model. The third version shows excellent accuracy. So from the other viewpoint, the Bauer formula can be improved by considering the RE and the f parameters.

Fig. 5 shows the graphical presentation of the accuracy of the three versions in case of Rt. The other investigated parameters show similar tendency in regression model.

Table 2 presents the values of the coefficients of the #3 version linear regression model for the investigated surface roughness parameters. The longitudinal Rsm parameter depends only the feed.

In conclusion, if the arc based geometric model is accepted as valid, the individual surface roughness parameters can be calculated numerically, based on the points of the generated profile or on the basis of the presented regression relationships. These values are theoretical, since they only take into account the geometric relationships and not other modifying conditions.

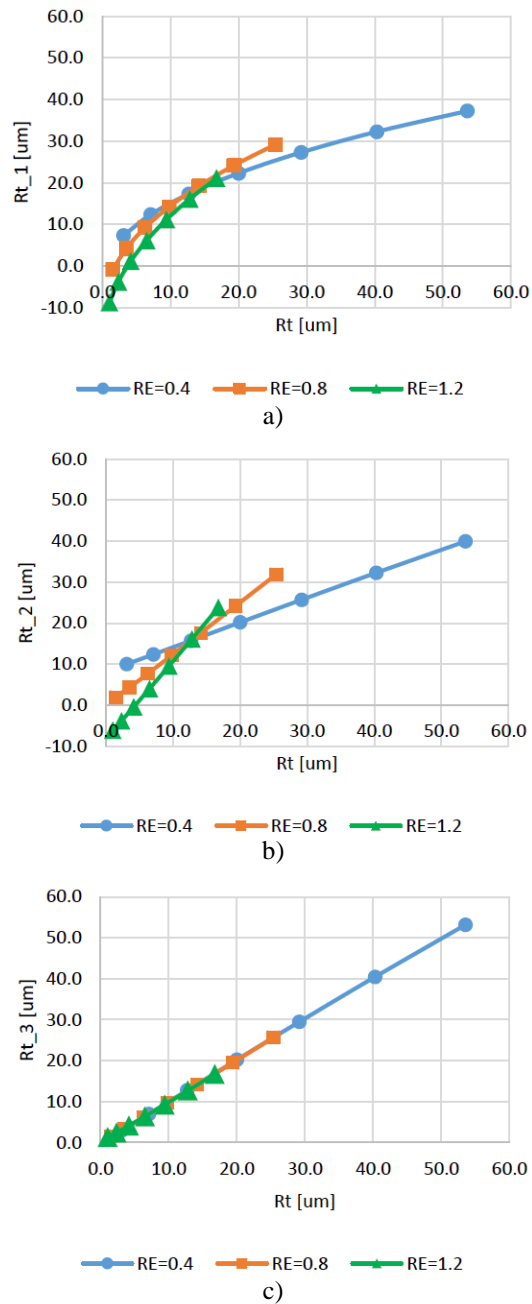


Figure 5. Comparing the simulation model with the regression model in case of Rt, a) #1 regression b) #2 regression, c) #3 regression.

Table 1. Values of the regression coefficients in case of Rt

Regression version	Coefficients					
		RE	f	f ²	Rt*	R ² (adj)
	C	C ₁	C ₂	C ₃	C ₄	
#1	5.457	-20.169	99.73	-	-	79.5
#2	16.643	-20.169	-6.81	213.1	-	80.5
#3	-0.198	0.858	-6.61	-	1.114	100.0

Table 2. Values of the regression coefficients.

Rx	Coefficients				R ² (adj)
	C	RE C ₁	f C ₂	Rt* C ₄	
Ra	-0.05428	0.23528	-1.81580	0.28826	100
Rz	-0.19840	0.85760	-6.61350	1.11367	100
Rq	-0.06237	0.26865	-2.07090	0.33433	100
Rt	-0.19840	0.85760	-6.61350	1.11367	100
Rp	-0.12318	0.53180	-4.10220	0.73694	100
Rv	-0.07570	0.32635	-2.51210	0.37675	100
Rsm	0	0	1000	0	100
Rsk	0.64229	-0.00131	0.02244	-0.00046	98.4
Rku	2.15084	-0.00107	0.03346	-0.00071	98.3

Table 3. Simulation and real data in case of V insert, RE=0.4, f=0.25.

	Ra	Rz	Rq	Rt	Rp	Rv	Rsm	Rsk	Rku
Simulation	5.16	20.03	5.99	20.03	13.33	6.70	250	0.64	2.14
Real (V insert)	4.95	20.57	5.65	21.78	12.82	7.75	253	0.47	2.03

IV. CONCLUSIONS

Fig. 6 shows a comparison of the simulated surface profile with a real surface profile as example in order to demonstrate the similarities and differences between the simulated and real surface profiles.

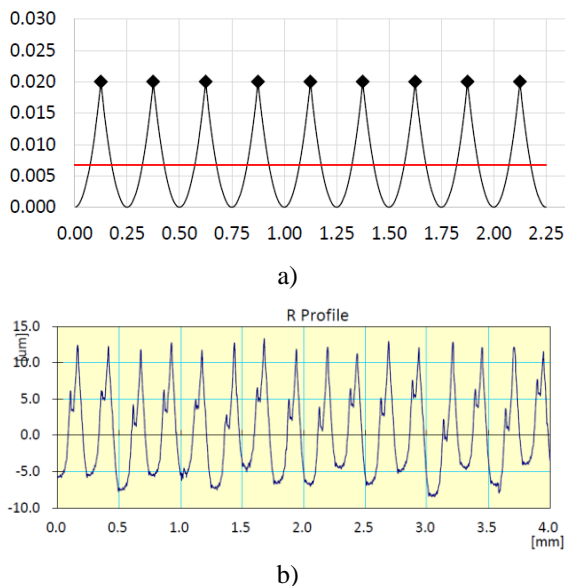


Figure 6. Surface profile (turning, Insert V, RE=0.4, f=0.25). a) Simulated surface profile. b) Real surface profile.

The simulated and the measured surface roughness parameters are close to each other (Table 3), but the surface profiles look different. The real profile contains random like elements, the RE curves can recognizable, but in the centre there is vertical and

horizontal deviations, and additionally the curve is not regular.

Based on the analysis of geometric-kinematic behaviour of the cutting, a theoretical surface model can be generated, and based on it, the surface roughness parameters can be calculated. Although the simulation and the real surface profile measure have similar results, the accuracy of the model should be improved. Based on the preliminary tests, the geometric model can be evolved by the systematic modification of the centre points of the nose radius and the value of the nose radius considering the machining circumstances, like the tool geometry and cutting parameters.

Based on this idea, we introduce the “equivalent replacement profile” (ERP), which results the same surface roughness parameters, like the real surface, but the look of the profile does not necessarily match the measured profile. Our research aim is to create the generation algorithm of the ERP model in case of turning. The base of the development is the results of analysing of real surfaces, which are created by several different tools and parameters. The presented geometric-kinematic model makes possible to modify the centre and the value of the nose radius, which has effect on the profile points and the surface roughness parameters. The core question of the further development is how can modify the profile element to reach the required accuracy (Fig. 7).

V. SUMMARY

Surface roughness is an important aspect of assessing the quality of the surfaces of mechanical components. Surface roughness design takes into account both operational and manufacturing aspects.

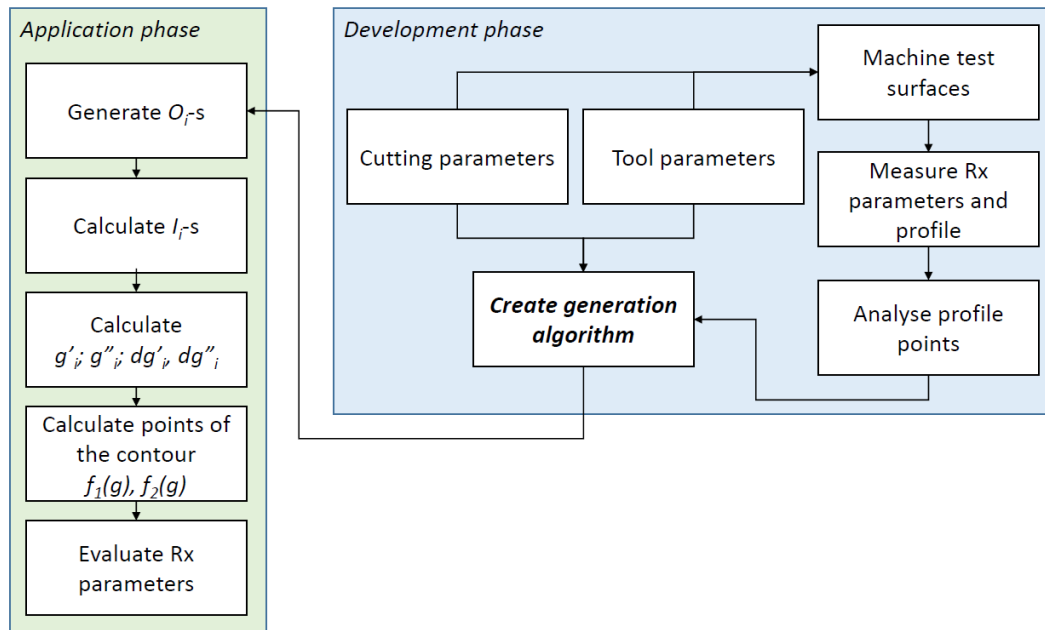


Figure 7. Development process of ERP model.

Surface roughness prediction is important in manufacturing process planning, for which there are several methods.

In this article, we examined the geometric-kinematic model. The circular arc-based geometric model was examined, and a simulation model was created that determines the coordinates of the profile points.

Based on the results, we made the following conclusions.

- The presented geometric-kinematic model of the machined surface by turning and the algorithm ensure the possibility of calculating every surface roughness parameter.
- Based on the simulation model a regression model was created, which improve the accuracy of the Bauer formulae and additionally contains the tool nose radius (RE), the feed (f). The regression model can predict the height parameters of the surface roughness.
- The Equivalent Replacement Profile is introduced, which similar to the real profile by the surface roughness parameters, but the look of the profile can be different.
- The presented geometric algorithm allows for systematic changes to the profile elements.

REFERENCES

- [1] Petropoulos, G.; Pandazaras, C.; Davim, J. Surface texture characterization and evaluation related to machining. In: Davim, J. (eds) Surface Integrity in Machining. Springer, London 2010 pp.37-66. https://doi.org/10.1007/978-1-84882-874-2_2
- [2] Bernardos P.G.; Vosniakos G.C. Predicting surface roughness in machining: a review. International Journal of Machine Tools & Manufacture 2003, 43:833–844. [https://doi.org/10.1016/S0890-6955\(03\)00059-2](https://doi.org/10.1016/S0890-6955(03)00059-2)

In the further research the profile generation algorithm will be developed based on statistical analysis of real surface profiles. The analysis of real surfaces allows the examination of systematic and random deviations. Our goal is to involve these deviations into the geometric-kinematic model.

AUTHOR CONTRIBUTIONS

S. Nuriddinov: Experiments, Data analysis, Writing, Visualization.

B. Mikó: Conceptualization, Review and editing, Supervision.

DISCLOSURE STATEMENT

The authors declare that they have no known competing financial interests or personal relationships that could have appeared to influence the work reported in this paper.

ORCID

Nuriddinov S. <http://orcid.org/0009-0009-6932-4234>

Mikó B. <http://orcid.org/0000-0003-3609-0290>

- [3] Chen, T. et al. An advanced approach for predicting workpiece surface roughness using finite element method and image processing techniques. *Machines* 2024 12:827.
<https://doi.org/10.3390/machines12110827>
- [4] Tomov, M.; Gecevska, V.; Vasilevska, E. Modelling of multiple surface roughness parameters during hard turning: A comparative study between the kinematical-geometrical copying approach and the design of experiments method (DOE), *Advances in Production Engineering & Management* 2022 17(1):75-88.
<https://doi.org/10.14743/apem2022.1.422>
- [5] Matras A. Surface roughness prediction in the hardened steel ball-end milling by using the artificial neural networks and Taguchi method. *Advances in Science and Technology Research Journal* 2024 18(1):184–194.
<https://doi.org/10.12913/22998624/177328>
- [6] Osan, A.R.; Drenta, R.F. Application of artificial neural networks in predicting surface quality and machining time. *Machines* 2025 13:561.
<https://doi.org/10.3390/machines13070561>
- [7] Mane, S.; Patil, R.B.; Al-Dahidi, S. (2025) Predictive modelling of surface roughness and cutting temperature using response surface methodology and artificial neural network in hard turning of AISI 52100 steel with minimal cutting fluid application. *Machines* 13:266.
<https://doi.org/10.3390/machines13040266>
- [8] Mahashar Ali J.; Murugan M. Surface roughness characterisation of turned surfaces using image processing. *International Journal of Machining and Machinability of Materials* 2017 19(4):394-406.
<https://doi.org/10.1504/ijmmm.2017.10006839>
- [9] Palásti-Kovács, B.; Sipos, S.; Bíró, Sz. The mysteries of the surface First part: The characteristic features of the microgeometry of the machined surface. *Acta Polytechnica Hungarica* 2014 11(5):5-24.
<https://doi.org/10.12700/aph.11.05.2014.05.1>
- [10] Sung A.N.; Ratnam M.M.; Loh W.P. Theoretical models for surface roughness in turning considering inclination and rake angles. *International Journal Surface Science and Engineering* 2018 12(3):171-192.
<https://doi.org/10.1504/ijsurfse.2018.094772>
- [11] Tomov M.; Kuzinovski M.; Cichosz P. Development of mathematical models for surface roughness parameter prediction in turning depending on the process condition. *International Journal of Mechanical Sciences* 2016 113:120-132.
<https://doi.org/10.1016/j.ijmecsci.2016.04.015>
- [12] Felhő, Cs.; Varga, Gy. Theoretical roughness modelling of hard turned surfaces considering tool wear. *Machines* 2022 10:188.
<https://doi.org/10.3390/machines10030188>
- [13] Mgherony, A.; Mikó, B.; Farkas, G. Comparison of surface roughness when turning and milling. *Periodica Polytechnica - Mechanical engineering* 2021 65(4):337-344 ISSN 0324-6051.
<https://doi.org/10.3311/ppme.17898>
- [14] Wang, B. et al. A predictive model of milling surface roughness. *The International Journal of Advanced Manufacturing Technology* 2020 108:2755–2762 (2020).
<https://doi.org/10.1007/s00170-020-05599-x>



This article is an open access article distributed under the terms and conditions of the Creative Commons Attribution NonCommercial (CC BY-NC 4.0) license

APPENDIX A

Calculation of the coordinates of intersection point by intersection of two circles.

Circle 1:

$$R_1^2 = (x - x_{o1})^2 + (y - y_{o1})^2 \quad (13)$$

$$R_1^2 = x^2 - 2 \cdot x \cdot x_{o1} + x_{o1}^2 + y^2 - 2 \cdot y \cdot y_{o1} + y_{o1}^2 \quad (14)$$

$$0 = x^2 + y^2 - 2 \cdot x \cdot x_{o1} - 2 \cdot y \cdot y_{o1} + x_{o1}^2 + y_{o1}^2 - R_1^2 \quad (15)$$

$$C_1 = x_{o1}^2 + y_{o1}^2 - R_1^2 \quad (16)$$

Circle 2:

$$R_2^2 = (x - x_{o2})^2 + (y - y_{o2})^2 \quad (17)$$

$$R_2^2 = x^2 - 2 \cdot x \cdot x_{o2} + x_{o2}^2 + y^2 - 2 \cdot y \cdot y_{o2} + y_{o2}^2 \quad (18)$$

$$0 = x^2 + y^2 - 2 \cdot x \cdot x_{o2} - 2 \cdot y \cdot y_{o2} + x_{o2}^2 + y_{o2}^2 - R_2^2 \quad (19)$$

$$C_2 = x_{o2}^2 + y_{o2}^2 - R_2^2 \quad (20)$$

Subtract Eq.(19) from Eq.(15):

$$0 = -2 \cdot x \cdot x_{o1} - (-2 \cdot x \cdot x_{o2}) - 2 \cdot y \cdot y_{o1} - (-2 \cdot y \cdot y_{o2}) + C_1 - C_2 \quad (21)$$

$$0 = 2x \cdot (x_{o2} - x_{o1}) + 2y \cdot (y_{o2} - y_{o1}) + C_1 - C_2 \quad (22)$$

$$x = \frac{C_2 - C_1 - 2y \cdot (y_{o2} - y_{o1})}{2 \cdot (x_{o2} - x_{o1})} \quad (23)$$

$$x = -y \frac{(y_{o2} - y_{o1})}{(x_{o2} - x_{o1})} + \frac{C_2 - C_1}{2 \cdot (x_{o2} - x_{o1})} \quad (24)$$

$$C_3 = \frac{(y_{o2} - y_{o1})}{(x_{o2} - x_{o1})} \quad (25)$$

$$C_4 = \frac{C_2 - C_1}{2 \cdot (x_{o2} - x_{o1})} \quad (26)$$

$$x = -y \cdot C_3 + C_4 \quad (27)$$

Substitute Eq.(27) into Eq.(15):

$$0 = (-y \cdot C_3 + C_4)^2 + y^2 - 2(-y \cdot C_3 + C_4)x_{o1} - 2yy_{o1} + C_1 \quad (28)$$

$$0 = y^2 C_3^2 - 2yC_3 + C_4^2 + y^2 + 2yC_3x_{o1} - 2C_4x_{o1} - 2yy_{o1} + C_1 \quad (29)$$

$$0 = y^2(C_3^2 + 1) - 2y(C_3 - C_3x_{o1} + y_{o1}) + (C_4^2 - 2C_4x_{o1} + C_1) \quad (30)$$

$$0 = a \cdot y^2 + b \cdot y + c \quad (31)$$

$$a = (C_3^2 + 1) \quad (32)$$

$$b = -2(C_3 - C_3x_{o1} + y_{o1}) \quad (33)$$

$$c = (C_4^2 - 2C_4x_{o1} + C_1) \quad (34)$$

Use the quadratic equation solution formula:

$$y_{1,2} = \frac{-b \pm \sqrt{b^2 - 4ac}}{2a} \quad (35)$$

$$x_{1,2} = -y_{1,2} \cdot C_3 + C_4 \quad (36)$$

Coordinates of the intersection point:

$$y_I = \frac{-b - \sqrt{b^2 - 4ac}}{2a} \quad (37)$$

$$x_I = -y_I \cdot C_3 + C_4 \quad (38)$$

APPENDIX B

Table 4. Simulated theoretical surface roughness parameters.

RE	f	Ra	Rz	Rq	Rt	Rp	Rv	Rsm	Rsk	Rku	Rt*
0.4	0.10	0.807	3.137	0.937	3.137	2.090	1.047	100	0.643	2.152	3.125
0.4	0.15	1.825	7.094	2.120	7.094	4.725	2.369	150	0.642	2.150	7.031
0.4	0.20	3.268	12.702	3.797	12.702	8.455	4.246	200	0.640	2.148	12.500
0.4	0.25	5.158	20.033	5.992	20.033	13.327	6.705	250	0.638	2.144	19.531
0.4	0.30	7.522	29.190	8.735	29.190	19.404	9.786	300	0.635	2.140	28.125
0.4	0.35	10.398	40.313	12.072	40.313	26.772	13.541	350	0.632	2.135	38.281
0.4	0.40	13.838	53.590	16.061	53.590	35.548	18.042	400	0.628	2.128	50.000
0.8	0.10	0.402	1.564	0.467	1.564	1.042	0.522	100	0.643	2.153	1.563
0.8	0.15	0.906	3.523	1.053	3.523	2.348	1.176	150	0.643	2.153	3.516
0.8	0.20	1.613	6.275	1.875	6.275	4.180	2.094	200	0.643	2.152	6.250
0.8	0.25	2.527	9.826	2.936	9.826	6.545	3.281	250	0.642	2.151	9.766
0.8	0.30	3.649	14.188	4.240	14.188	9.449	4.739	300	0.642	2.150	14.063
0.8	0.35	4.985	19.375	5.791	19.375	12.901	6.474	350	0.641	2.149	19.141
0.8	0.40	6.537	25.403	7.595	25.403	16.911	8.493	400	0.640	2.148	25.000
1.2	0.10	0.268	1.042	0.311	1.042	0.694	0.348	100	0.643	2.153	1.042
1.2	0.15	0.603	2.346	0.701	2.346	1.563	0.783	150	0.643	2.153	2.344
1.2	0.20	1.073	4.174	1.247	4.174	2.781	1.393	200	0.643	2.153	4.167
1.2	0.25	1.678	6.528	1.950	6.528	4.350	2.179	250	0.643	2.152	6.510
1.2	0.30	2.420	9.412	2.812	9.412	6.270	3.141	300	0.643	2.152	9.375
1.2	0.35	3.299	12.829	3.833	12.829	8.546	4.283	350	0.642	2.152	12.760
1.2	0.40	4.316	16.784	5.016	16.784	11.180	5.604	400	0.642	2.151	16.667

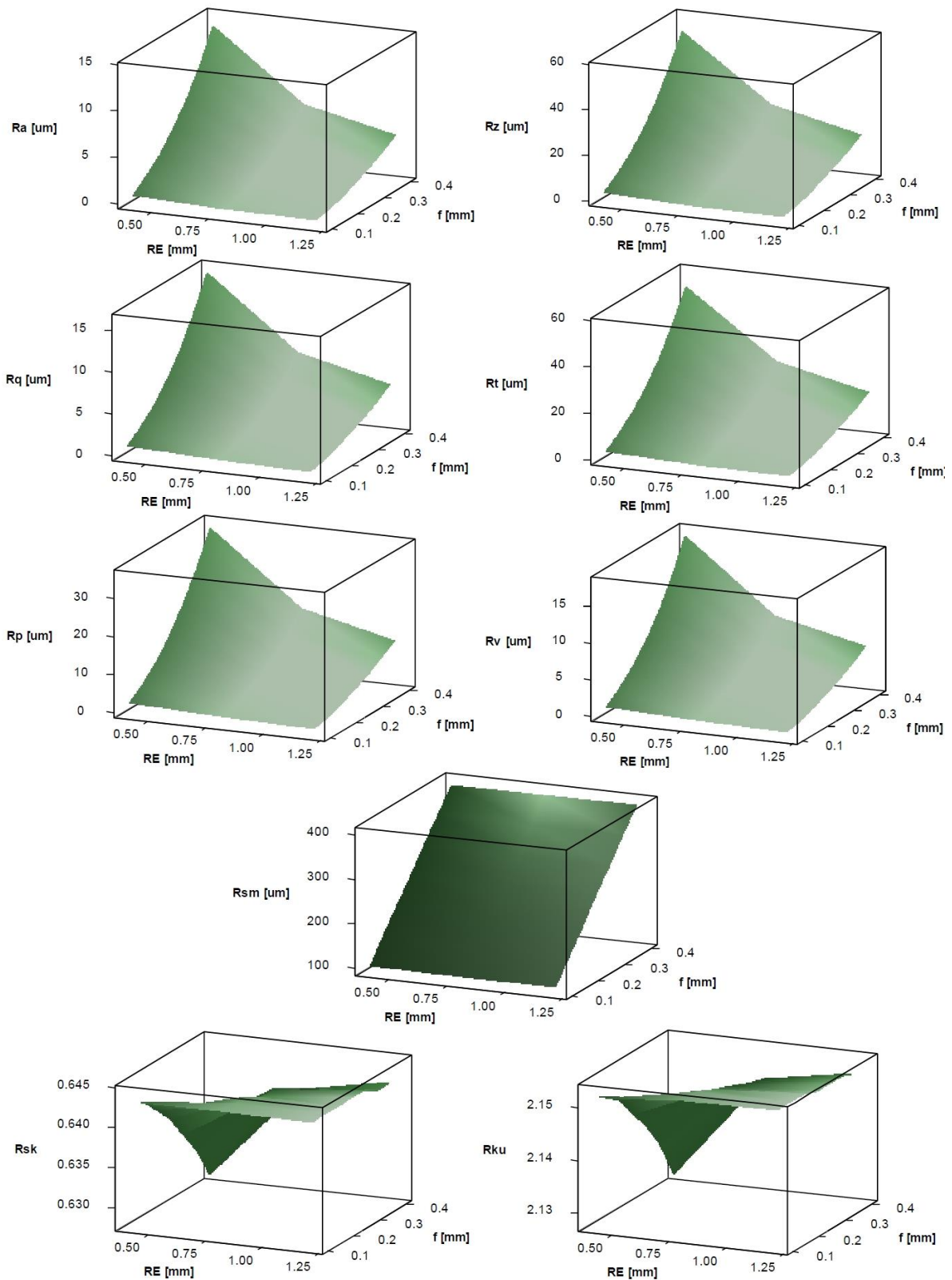


Figure 8. The results of the simulation.